Available online at www.sciencedirect.com
SCIENCE DIRECT
Enzyme and Microbial Technology 39 (2006) 149–157
ENZYME AND MICROBIAL TECHNOLOGY
www.elsevier.com/locate/emt

Manipulation of the physiology of clavulanic acid biosynthesis with the aid of metabolic flux analysis

Michael E. Bushell *, Samantha Kirk, Hong-Juan Zhao, Claudio A. Avignone-Rossa

Microbial Science Group, School of Biomedical and Molecular Sciences, University of Surrey, Guildford, Surrey, GU2 7XH, UK

Received 12 July 2005; received in revised form 4 January 2006; accepted 12 January 2006

Abstract

Feeding a chemostat culture of *Streptomyces clavuligerus* with a combination of amino acids, formulated with the aid of metabolic flux analysis (MFA), resulted in an 18-fold increase in antibiotic (clavulanic acid) yield compared to the non-fed control. MFA of cultures fed with single amino acids was consistent with availability of the C_3 precursor of clavulanic acid limiting antibiotic yield in phosphate-limited cultures, suggesting that the urea cycle, present in this species, was capable of providing excess C_5 precursor. Fluxes through reactions leading to biosynthesis of precursors of the C_3 moiety of the clavulanic acid molecule, correlated with flux to clavulanic acid when the dilution rate was varied.

Keywords: Metabolic flux; Streptomyces; Clavulanic acid

1. Introduction

Clavulanic acid is a clinically-important antibiotic produced by *Streptomyces clavuligerus* [1]. The interest in obtaining higher yields of the product has led to several studies on the genetics, physiology, and biochemistry of the pathways involved in the antibiotic biosynthesis in particular, and in secondary metabolism, in general. The generic status of clavulanic acid provides an incentive to explore generally-applicable approaches to increasing product yield by rational culture design.

Metabolic flux analysis has been applied to bioprocesses for penicillin [2], vitamins [3], amino acids [4–6], proteins [7,8] and recombinant DNA for gene therapy [9]. In addition, fluxes through amino acid biosynthetic reactions have been analysed with regard to the production of transglutaminase by *Streptoverticillium mobaraense* [7] and serine alkaline protease by *Bacillus licheniformis* [8]. However, few studies have applied metabolic flux analysis to the design of mutants for enhanced antibiotic production. This is surprising as the technique facilitates the identification of the pathway fluxes that are significantly correlated with the synthesis of bioproducts of interest [10–12], providing the potential for rational strain or process design for maximum product yield.

Amino acids have important regulatory roles in the nitrogen metabolism of *Streptomyces* in general, and in the synthesis of clavulanic acid and cephamycin by *S. clavuligerus* in particular. It has been reported that lysine stimulates production of β-lactam antibiotics by *S. clavuligerus* [13], whereas alanine inhibits the synthesis of cephalosporin [14]. Amino acids are also precursors of a number of antibiotics, including clavulanic acid [15] and the cephamycins [13,16]. However, the concentrations of antibiotics produced by non-industrial strains are comparatively low (e.g. Bushell and Fryday [17]), and, therefore, carbon fluxes through amino acid precursor pools will be proportionately lower than those observed in protein bioproduct synthesis. In this paper, we propose that MFA in antibiotic-producing cultures can, nevertheless, be employed to identify those intermediary metabolites whose production rates are critical to attainment of maximum yields.

We have applied metabolic flux analysis to chemostat cultures of *S. clavuligerus* growing under different nutrient limitations [18]. Our results showed that the nature of the nutrient limiting growth affected the availability of the precursors of clavulanic acid, thereby affecting clavulanic acid titres. It seemed that a high carbon flux through anaplerotic metabolism may be responsible for the stoichiometric limitation of a C_3 precursor. We have also reported a novel use of cluster analysis for the identification of intermediary metabolites that are produced at rates closely correlated with those of antibiotic biosynthesis [19]. This information was used to devise culture feeds resulting in enhanced

* Corresponding author.
E-mail address: m.bushell@surrey.ac.uk (M.E. Bushell).

0141-0229/$ – see front matter © 2006 Published by Elsevier Inc.
doi:10.1016/j.enzmictec.2006.01.017

production of clavulanic acid. The feeding strategies apparently alleviated a rate-limiting supply of the C_3 precursor of clavulanic acid. These observations were consistent with those of Chen et al. [20], who interpreted the results of their feeding experiments to indicate a dependence on availability of C_3 precursor. In *S. clavuligerus*, ornithine is converted to arginine (via a sequence analogous to the mammalian urea cycle) prior to incorporation into clavulanic acid [21]. The remainder of the clavulanic acid molecule is derived from the C_3 precursor [22,23], which has been identified to be glyceraldehyde 3-phosphate [24] (Fig. 2). We demonstrated that the distribution of carbon flux through catabolic pathways in *Streptomyces lividans* is dependent on growth rate as well as nutrient availability, increasing growth rates leading to increased flux through glycolysis and the pentose phosphate pathway [25].

In this paper, we present data from chemostat cultures of *S. clavuligerus*, and an example of the predictive use of mfa to design amino acid feed formulations for enhanced clavulanic acid yield. A detailed metabolic network is presented, together with the calculation of significant intermediary metabolite fluxes and the estimation of their influence on clavulanic acid production. The procedure is comparatively simple as it does not require radiotracer analysis and could be readily employed in a process improvement laboratory to gain a significant increase in product yield.

2. Materials and methods

2.1. Strains and culture media

A single spore isolate of *S. clavuligerus* NRRL 3585 was obtained from GSK and used throughout this work. The P-limited chemically defined culture medium for *S. clavuligerus* contained: ($g\,l^{-1}$, in reverse osmosis purified water) glycerol 60.0, NH_4Cl 7.0, KH_2PO_4 0.1, MOPS, 21.0. The medium was supplemented with trace elements, by addition ($10\,ml\,l^{-1}$ of medium) of a solution containing ($g\,l^{-1}$): $MgSO_4{\cdot}7H_2O$ 25.0, $FeSO_4{\cdot}7H_2O$ 2.5, $CuCl_2$ 0.053, $CoCl_2$ 0.055, $CaCl_2{\cdot}2H_2O$ 1.38, $ZnCl_2$ 1.04, $MnCl_2$ 0.62, Na_2MoO_4 0.03. The pH of this stock solution was adjusted to 7.0, using HCl. In the amino acid supplemented chemostats, the corresponding amino acids were added at concentrations of 10 mM. The medium was sterilized by filtration through a sterile cartridge. The pH was adjusted to 7.0 with 5 M KOH before filtration.

2.2. Preparation of inocula

S. clavuligerus cultures were routinely maintained on SV2 agar [19]. Agar plugs were aseptically cut out from sporing plates and transferred to cryotubes containing 1 ml of a 10% glycerol in Brain–Heart infusion broth. The spore stocks were kept at −20 °C until inoculation. The content of a cryotube was transferred to 250 ml baffled Erlenmeyer flasks containing 25 ml SVD medium, and incubated at 30 °C for 48 h on a rotary shaker at 250 rev/min. Erlenmeyer flasks containing 25 ml P-limited minimal medium were inoculated with 2.5 ml of the culture, and incubated for 24 h at the same conditions. Chemostats were inoculated with this culture at a rate of 5% (v/v).

2.3. Bioreactor culture

Chemostat cultures were performed in a 2.5 l B. Braun bioreactor (B. Braun, Sheffield, UK), with a working volume of 1 l. The aeration regime was 2 vvm, and the stirring rate was 750 rev/min and employed a single Rushton turbine impellor, located just above the sparger. Temperature was controlled at 30 °C, and pH at 6.8 ± 0.2 by the automatic addition of 0.5 M KOH or 0.5 M HCl. Exhaust gas was analysed by using infrared (CO_2) and paramagnetic (O_2) gas analysers and airflow was estimated using a mass flow meter. After inoculation, cells were grown batchwise for 24 h before starting the addition of fresh medium. The medium was supplied by a peristaltic pump, with flow rates set to obtain the desired dilution rates. During the experiments, dissolved oxygen concentration remained above 70% and nutrient pulse additions ensured that cultures were not oxygen-limited.

2.4. Sampling

Four volume changes were allowed before sampling, in order to ensure steady states had been reached. This was confirmed by constancy in O_2 consumption and CO_2 production. Exhaust gas analysis was performed before sampling. Culture samples (max 50 ml) were withdrawn from the chemostat by a pipe submerged in the culture broth, and received in a sterile bottle kept in an ice-bath. In order to calculate accurately the nutrient consumption rates, samples of the fresh medium were taken from the reservoir simultaneously with the culture sampling.

2.5. Biomass determination

Culture samples (10 ml) were collected on pre-dried membrane filters (Gelman 0.45 μm), and washed with distilled water (3× 10 ml). The filters were dried in a microwave oven (700 W, 2× 5 min). After cooling down in a dessicator, filters were weighed to obtain the biomass dry weight. Triplicate biomass concentrations were determined. Filtrates were collected and frozen for extracellular metabolite assays.

2.6. Clavulanic acid

Antibiotic concentrations were evaluated by HPLC, following the procedure already described [26].

2.7. Analytical determinations

A glycerol enzymatic assay (TC Glycerol, Bohringer) was employed for the determination of glycerol in the supernatants and in the fresh medium. Total extracellular polysaccharides were assayed by the anthrone method [27]. Amino acid concentrations were measured by HPLC (Waters PicoTag).

Protein was determined using the method of Lowry et al. [28]. Cellular composition was estimated against a standard curve of bovine serum albumin ($25–200\,\mu g\,ml^{-1}$). The protein content of samples from our experiments was within the range 40–50% of dry cell mass. Samples were solubilized in hot 1 M sodium hydroxide.

Carbohydrate was determined by the phenol/sulphuric acid method [29]. Cellular composition was estimated against a standard curve of glucose ($10–200\,\mu g\,ml^{-1}$). The carbohydrate content of samples was within the range 10–15% of dry cell mass, therefore $1250\,\mu g\,ml^{-1}$ of freeze-dried biomass was used in order to obtain a carbohydrate concentration that would be within the mid-standard range.

The lipid content was determined using the chloroform:methanol extraction method [30]. Solvent extraction was applied to freeze-dried biomass and the mass of lipid was then measured.

DNA was determined using the diphenylamine method of Burton [31] using a hot perchloric acid extraction of freshly-harvested biomass. Samples were estimated against a calf-thymus DNA standard solutions ($100–500\,\mu g\,ml^{-1}$).

The RNA content was determined using an oricinol-based procedure [32] on the same extract that was used for DNA extraction (see above) against calf liver RNA standard solutions ($100–500\,\mu g\,ml^{-1}$).

2.8. Other culture supernatant analysis

Nutrient concentrations were measured using an RQ-reflectoquant analyser (Merck/VWR International).

Ammonium was determined using a colorimetric assay kit (VWR International: 31914 3E). A 1 ml sample was used with two drops of the reagent

supplied. In this assay, NH_4^+ ions react with Nessler's reagent resulting in a yellow–brown compound, the concentration of which can be determined reflectometrically. The detection limits are 20–180 mg l^{-1} NH_4^+.

Phosphate was determined using a colorimetric assay kit (VWR International: 31923 3F). A 1 ml sample was used with two drops of reagent supplied. Orthophosphate ions PO_4^{3-} and molybdate ions form molybdophosphoric acid in a solution acidified with sulphuric acid. The resulting molybdophosphoric acid is then reduced to phosphomolybdenum blue (PMB) – the concentration of which may be measured reflectrometrically, and hence the phosphate concentration can be determined. The detection limits of the method are 5–120 mg l^{-1} PO_4^{3-}.

2.9. The stoichiometric bioreaction network

The main metabolic pathways (glycolysis, tricarboxylic acid cycle, and pentose phosphate pathway), as well as the reactions for the synthesis of all precursors involved in biomass and clavulanic acid production, were included in the biochemical network developed for *S. clavuligerus*. The equations included the requirements for cofactors such as ATP and NAD(P)H. Biomass was composition was determined experimentally (in C-mole/C-mole biomass): protein, 0.52; carbohydrates, 0.13; lipids, 0.13; DNA, 0.03; RNA, 0.19 which agrees with published values [33–35]. No significant variation was observed when growth rate was changed.

The equations for the main metabolic pathways are those recognized to be present in most species of *Streptomyces* [36–38]. The Entner-Doudoroff pathway and the glyoxylate shunt have never been reported in *Streptomyces*. It has been reported that the oxidative step of the pentose phosphate pathway is not active in *E. coli* grown with glycerol as the carbon source [39]. This has been assumed to be the case for *S. clavuligerus* in constructing the model. Only one anaplerotic reaction has been considered in the metabolic network model, namely the carboxylation of phosphoenol pyruvate (Appendix A reaction 39), following reports stating that this is the only anaplerotic reaction found to be present in *Streptomyces* species [40]. We have assumed the presence of nicotinamide nucleotide transhydrogenase, which catalyzes the reversible conversion of NADH into NADPH (Appendix A, reaction 52). The reactions for amino acid biosynthesis are those considered to be present in most microorganisms [41]. Several papers have reported that *S. clavuligerus* possesses enzyme activities related to the urea cycle, including arginase activity [42] and ornithine carbamoyltransferase [43]. For this reason, the reactions corresponding to the urea cycle have been included in the stoichiometric model (Appendix A, reactions 53–56). The stoichiometry of clavulanic acid synthesis (Appendix A, reaction 57) has been formulated using reported information [44–46].

The complete stoichiometric bioreaction network used in this study is presented in Appendix A.

2.10. Amino acid feeds

Isoleucine, aspartate, threonine, arginine and glutamate were each added to the medium at a concentration of 10 mM. In general, an increase in the pool size of a particular amino acid will repress its own biosynthetic pathway (see Hodgson [40]). Therefore, in each case, the stoichiometric model was modified assuming that the carbon flux through the biosynthesis of the amino acid being fed was negligible. The equation representing the biosynthesis of the amino acid concerned was replaced by an equation representing its uptake (Appendix A). A dilution rate of 0.03 h^{-1} was chosen for the amino acid feeding experiments, as this had resulted in the highest clavulanic acid yield when dilution rate was varied.

2.11. Reproducibility and replication of experiments

All experimental data were obtained from single cultures. Experiments were carried out in triplicate to ensure that the trends and relationships observed in the culture parameters measured were reproducible. Individual assays were replicated four-fold. Experiments were rejected where a χ^2-test indicated significant differences between replicates.

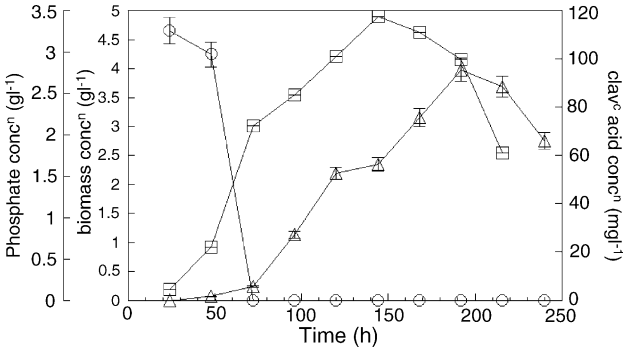

Fig. 1. Batch bioreactor culture of *Streptomyces clavuligerus* showing biomass (squares), phosphate (circles) and clavulanic acid (triangles) concentrations as a function of time in phosphate-limited batch culture.

3. Results and discussion

3.1. Response to phosphate-limited conditions

Production of antibiotic, relative to growth and phosphate limitation, was consistent with secondary metabolite production dynamics for clavulanic acid (Fig. 1). Our previous study [18] demonstrated that maximum yield of antibiotic is obtained under phosphate limitation, where availability of the C_3 precursor is the limiting factor for antibiotic yield. We further concluded that, under carbon limitation, it is the availability of the C_5 precursor of clavulanic acid that limits production. Carbon limitation apparently restricted the capacity for anaplerotic metabolism, minimising the potential for extensive TCA cycle-derived biosynthesis (the first stage in production of the C_5 precursor). Nitrogen limitation presumably restricts amino acid biosynthesis (the next stage).

3.2. Extracellular product formation

Clavulanic acid production decreased with dilution rate (Table 1) which is a typical secondary metabolite production pattern [47] and consistent with other work [48]. Polysaccharides were detected in the supernatants at every dilution rate tested, which is consistent with the presence of excess carbon source in these phosphate-limited cultures. There is very good ^{13}C evidence that polysacchardes are formed from cycling between two glucose-6-phosphate molecules and one fructose-6-phosphate molecule, releasing one glycosidic polysaccharide precursor with each turn of the cycle [49]. This does not require involvement of the PP pathway as glycerol is converted to glucose-6-P and fructose-6-P via glyceraldehyde phosphate. However, no excretion of organic acids was detected. Carbon balances were within the limits ($100 \pm 3\%$) in all of the experiments reported here. Clavulanic acid yields increased from 0.04 mg_{clav} $g_{glycerol}^{-1}$ ($D = 0.1\ h^{-1}$) to 0.58 mg_{clav} $g_{glycerol}^{-1}$ ($D = 0.03\ h^{-1}$). These yield values are similar to those obtained previously, in P-limited batch cultures using a different strain and medium formulation [19]. Flux to clavulanic acid varied between 0.23 C-mole l^{-1} h^{-1} ($D = 0.03\ h^{-1}$) and 0.06 C-mole l^{-1} h^{-1} ($D = 0.10\ h^{-1}$). Antibi-

Table 1
Nutrient input and bioproduct output in chemostat culture of *Streptomyces clavuligerus* at various dilution rates

Dilution rate (h^{-1})	Biomass production rate ($g\,l^{-1}\,h^{-1}$)	Specific glycerol consumption rate ($g\,g^{-1}\,h^{-1}$)	Specific clavulanic acid production rate ($mg\,g^{-1}\,h^{-1}$)	Specific polysaccharide production rate ($g\,g^{-1}\,h^{-1}$)	Specific CO_2 production rate ($g\,g^{-1}\,h^{-1}$)	Specific O_2 consumption rate ($g\,g^{-1}\,h^{-1}$)
0.03	0.036	0.45	0.32	0.12	0.39	0.41
0.05	0.053	0.60	0.27	0.18	0.52	0.53
0.07	0.071	0.93	0.15	0.45	0.60	0.63
0.10	0.090	2.18	0.10	0.95	1.63	1.71

otic yield values relative glycerol consumption are quoted, as these enable comparisons across the different experiments to be made.

3.3. Intracellular carbon flux through major catabolic pathways

Intracellular fluxes were estimated by solving the bioreaction network equations using observed extracellular metabolite accumulation rates (Table 1) and rates of biosynthesis of macromolecules. The flux of carbon through the pentose phosphate pathway (data not shown) was very low (around 1% of the input), and glycerol was catabolized mainly through glycolysis (92–98%). This is consistent with the observed comparatively low biomass yield, as the pentose phosphate pathway is a major source of precursors for biomass synthesis. The model does not assume the oxidative step converting glucose 6-phosphate into ribulose 5-phosphate, and, therefore, assumes that the TCA cycle

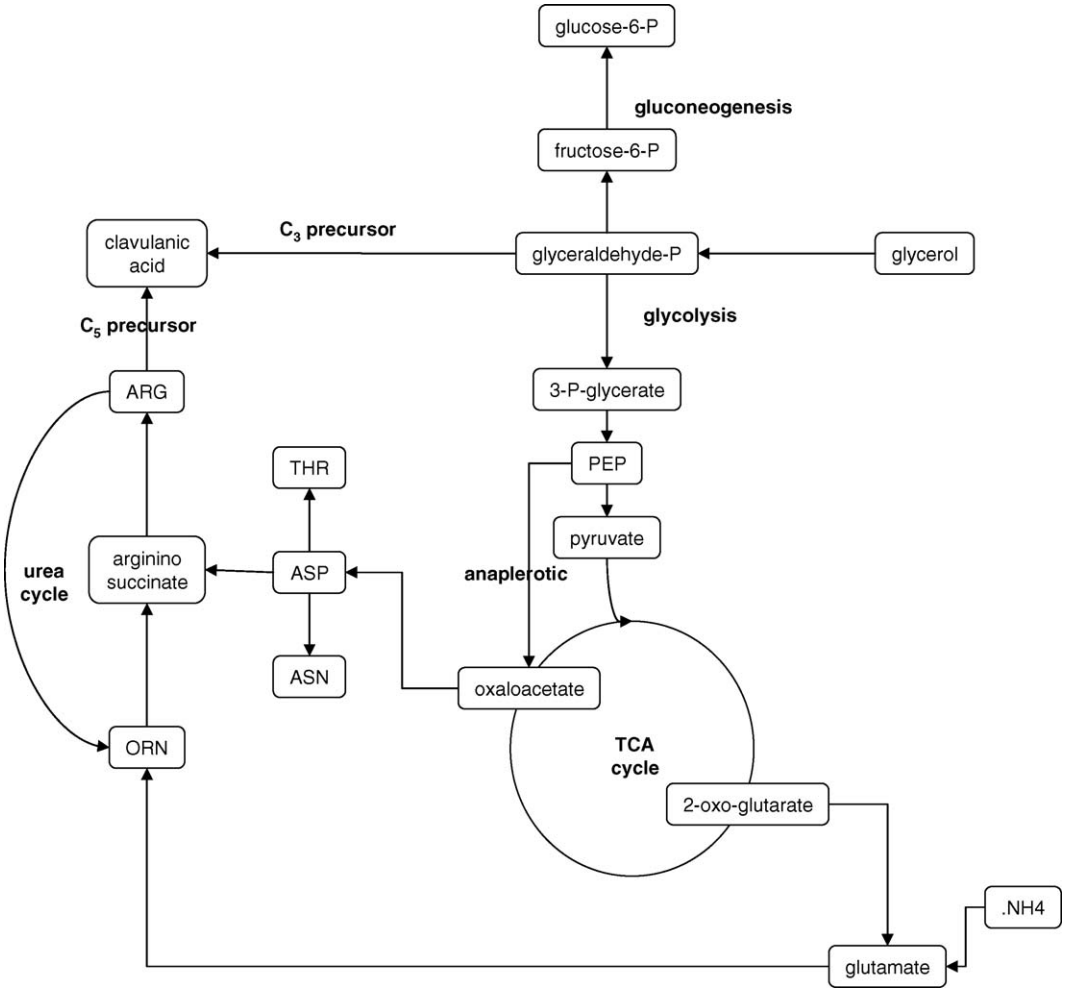

Fig. 2. Postulated biosynthetic scheme for clavulanic acid production in *S. clavuligerus*, illustrating major carbon fluxes discussed in this paper (many linear, non-branching steps omitted).

Table 2
Reactions in the network whose flux values correlate ($R \geq 0.85$) with those of clavulanic acid biosynthesis as a function of dilution rate

Reaction number	Reaction	Correlation coefficient with reaction 57
57	Glyceraldehyde-3-phosphate + 2 arginine + 0.667NADPH + 0.333FAD → 3 clavulanic acid + 0.667NADP + 0.333FADH	
4	α-Glycerophosphate + 0.333ADP + 0.333NAD → glyceraldehyde-3-phosphate + 0.333ATP + 0.333NADH	0.88
5	Glyceraldehyde-3-phosphate ↔ phosphoenolpyruvate	0.85
34	0.6 Phosphoenolpyruvate + 0.4 erythrose-4-P + 0.1NADPH + 0.1ATP + 0.5 glutamate → 0.9 phenylalanine + 0.5 α-ketoglutarate + 0.1CO_2 + 0.1 ADP + 0.1 NADP	−0.85
2	α-Glycerophosphate + 0.167ADP ↔ fructose-6-phosphate + 0.167ATP	−0.86
50	2FADH + O_2 + 2ADP → 2ATP + 2FAD	−0.88
17	Ribulose-5-P ↔ xylose-5-P	−0.89
35	0.6 Phosphoenolpyruvate + 0.4 erythrose-4-P + 0.1NADPH + 0.1ATP + 0.5 glutamate	−0.98
7	Pyruvate + 0.333NAD → 0.667 acetyl-Co-A + 0.333 CO_2 + 0.333NADH	−0.99
42	0.555 Glutamine + 0.555 ribose-5-P + 0.666ATP + 0.444 aspartate + 0.111NAD ↔ UTP + 0.666ADP + 0.555 glutamate + 0.111NADH	−0.99

is the only source of NADPH. The flux through the TCA cycle was approximately 50% of the carbon input for every dilution rate tested.

3.4. Urea cycle

The flux through the urea cycle (Fig. 2) was found to be high (∼20% of the carbon input) and constant over the whole range of dilution rates (data not shown). This is consistent with the suggestion that the cycle has a major role in nitrogen metabolism in this species. It has been reported that some urea cycle intermediates participate in clavulanic acid synthesis [15,34], but changes in clavulanic acid production rates did not correlate with the fluxes through the cycle. This agrees with our previous assertion that urea cycle activity provides an excess in the supply of arginine, the C_5 precursor, for clavulanic acid biosynthesis, under phosphate limitation [18]. The presence of a urea cycle in a prokaryote is unusual but not unprecedented [50].

3.5. Effect of dilution rate on fluxes

Maximum flux to clavulanic acid (Appendix A and Table 2, reaction 57) was obtained at the minimum dilution rate ($0.03\,h^{-1}$). The response of fluxes in reaction 57 to changing dilution rate was compared to that of all of the other reactions by calculating the correlation coefficients, comparing the reaction 57 dataset with the datasets for all of the other reactions. Metabolic fluxes of each of the 57 reactions in the network was plotted against that of clavuligerus biosynthesis or the four dilution rates studied. The correlation coefficient was calculated for each plot and all the reactions were ranked according to their correlation coefficient with reaction 57. Of the reactions whose correlation coefficients were greater than 0.85 and whose fluxes linked to reaction 57 or its precursors (Fig. 3), the most significant positive correlation (Table 2) was observed from reaction 4 (Fig. 3) the production of the clavulanic acid C_3 precursor, glyceraldehyde-3-phosphate from α-glycerophosphate (Table 2). No significant correlations were obtained with reactions whose fluxes linked directly to arginine, the C_5 precursor, which is consistent with our suggestion that arginine biosynthesis is saturated for clavulanic acid production under phosphate-limited conditions [18,19]. Flux through reaction 5, the reversible biosynthesis of glyceraldehyde-3-phosphate from phosphoenol pyruvate (Fig. 3) was also positively correlated with antibiotic production. This is probably a reflection of the high rate of production of glyceraldehyde-3-phosphate, which allows fluxes to both PEP and the clavulanic acid to be raised under P limitation.

Significant negative correlation with clavulanic acid biosynthetic flux was obtained from reactions that competed for precursors of glyceraldehyde-3-phosphate (Table 2), such as reactions 35, 34 and 2 (Fig. 3). A strong negative correlation ($R = -0.99$) was obtained with reaction 42 (a series of reactions leading to UTP biosynthesis, resulting in the formation of glutamate from

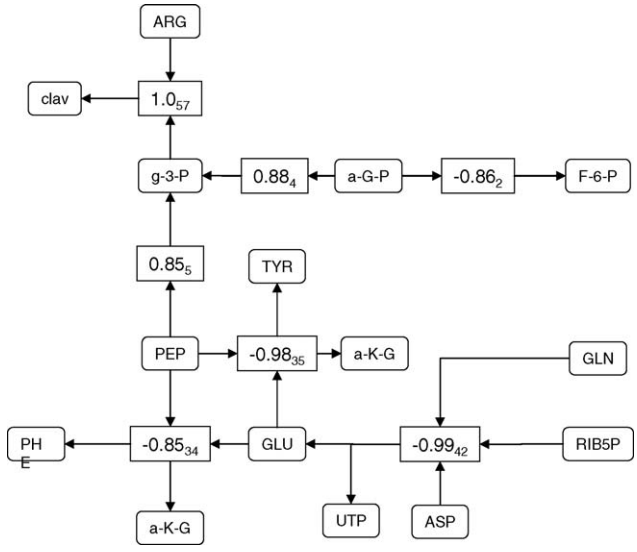

Fig. 3. A subset of bioreactions in the model, showing only those connected to clavulanic acid precursor biosynthesis, and whose fluxes are correlated ($r \geq 0.85$) with reaction 57. Large figures in boxes indicate the correlation coefficient observed for the individual reactions and subscripts indicate the reaction number (see also Table 2). Results from P-limited chemostat cultures grown over a range of dilution rates.

Table 3
Biomass and clavulanic acid production rates and selected intracellular fluxes in chemostat cultures (0.03 h^{-1}) of *S. clavuligerus* subject to single amino acid feeds

Amino acid feed	Biomass production rate ($g\,l^{-1}\,h^{-1}$)	Specific clavulanic acid production rate ($mg\,g^{-1}\,h^{-1}$)	Intracellular flux through reaction 2 (C-mole $l^{-1}\,h^{-1}$)	Intracellular flux through reaction 7 (C-mole $l^{-1}\,h^{-1}$)	Intracellular flux through reaction 34 (C-mole $l^{-1}\,h^{-1}$)	Intracellular flux through reaction 42 (C-mole $l^{-1}\,h^{-1}$)	Intracellular flux through reaction 57 (to clavulanic acid) (C-mole $l^{-1}\,h^{-1}$)
None	0.036	0.32	0.45	87.19	0.41	0.17	0.23
THR	0.046	0.55	−3.98	87.80	0.35	1.12	0.25
ARG	0.052	0.46	−2.23	85.13	0.04	1.74	0.21
ASP	0.038	0.35	−8.49	82.53	0.64	1.70	0.16
GLU	0.039	0.33	−5.68	82.59	0.71	1.79	0.15
ASN	0.046	0.31	−9.45	84.54	0.64	1.84	0.14
ILE	0.031	0.51	−8.44	85.12	1.40	0.42	0.23

Maximum standard error observed was 4.5% (flux through reaction 57 with isoleucine feed) standard error values omitted for clarity.

Table 4
Biomass and clavulanic acid production rates and selected intracellular fluxes in chemostat cultures (0.03 h^{-1}) of *S. clavuligerus* subject to multiple amino acid feeds

Amino acid feed	Biomass production rate ($g\,l^{-1}\,h^{-1}$)	Specific clavulanic acid production rate ($mg\,g^{-1}\,h^{-1}$)	Clavulanic acid yield ($mg_{clav}\,g^{-1}_{glycerol}$)	Intracellular flux through reaction 34 (C-mole $l^{-1}\,h^{-1}$)	Intracellular flux through reaction 42 (C-mole $l^{-1}\,h^{-1}$)	Intracellular flux through reaction 57 (to clavulanic acid) (C-mole $l^{-1}\,h^{-1}$)
None	0.036	0.32	0.58	0.41	0.17	0.23
ARG/ASP/THR	0.060	1.33	2.49	0.32	0.25	1.17
ASN/ARG/ASP/THR	0.049	1.61	3.02	0.46	1.01	1.6

glutamine during an intermediate step resulting in carbamoyl phosphate biosynthesis). If the primary influence of reaction 42 on clavulanic acid biosynthesis is the net glutamate biosynthesis, the correlation may be negative because the provision of glutamate fuels competing reactions 35 and 34. The flux through reaction 2 changes from positive to negative, presumably as a result of the same carbohydrate cycles referred to earlier [49].

3.6. Effect of amino acid feeds

All amino acid feeds resulted in a reversal in flux in reaction 2 (Fig. 3, Table 3) however, this was offset, to varying degrees by an increase in flux through reaction 34 (Fig. 3). When considering the amino acid fed cultures, flux through reaction 42 again correlated negatively ($R = -0.86$) with flux to clavulanic acid production. A positive correlation was obtained with reaction 7 ($R = 0.86$) suggesting that the major beneficial effect of feeding the amino acids was derived from an increase in the rate of entry of C_2 precursor (acetylCoA) into the TCA cycle. Our previous work [19] showed that the target amino acid intra-cellular pool size was increased by introduction of the appropriate feed, indicating that the fed nutrients entered the biosynthetic network rather than being subjected to a degradation pathway. The feeding concept was explored further by feeding combinations of amino acids.

3.6.1. Effect of feeding combinations of amino acids

The concept that clavulanic acid biosynthesis was dependent on supply of the C_3 precursor and, therefore, potentially influenced by the competing demands of glycolysis, providing biosynthetic input to the TCA cycle was explored by feeding with combinations of amino acids derived from oxaloacetate. An aspargine/arginine/threonine feed increased flux into clavulanic acid five-fold and an aspargine/arginine/threonine/aspartate feed increased it by seven-fold.

The clavulanic acid specific production rate and yields increased accordingly (Table 4). Specific production rates increased 4.3- and 5.2-times, whereas yields increased 13- and 18-times.

4. Conclusions

The results are consistent with the notion that the synthesis of clavulanic acid is limited by the availability of the C_3 precursor, resulting from the species' limited ability to assimilate glucose [51], necessitating the use of glycerol as carbon source. It appears that competition from other C_3-utilising pathways can influence this availability. Consistent with this concept is the observation that feeding those amino acids whose biosynthesis require oxaloacetate as a precursor, promoted a clavulanic acid yield in excess of 10 times that of the non-supplemented culture.

This work demonstrates the potential for rational feed design for antibiotic production based on metabolic flux analysis. As the feeds responsible for yield enhancement are not precursors, they are not obvious and could only have been identified using a predictive model. Future work will include further analysis of the stoichiometric network using elementary modes analysis and metabolic control analysis to study regulation.

Acknowledgement

We are grateful to the BBSRC for financial support for this work.

Appendix A. The stoichiometric bioreaction network used in this study

Metabolic flux analysis involves the measurement of extracellular metabolites and a Pseudo steady state approximation for intracellular metabolites (that is, the accumulation rates of intracellular metabolites is assumed to be zero). To simplify the stoichiometric network, several assumptions have to be made: (i) the network considers only metabolites involved in branching points. The pseudo steady state assumption states that all reactions in a linear sequence must occur at the same rate; (ii) those metabolites freely interconvertible are represented as a single metabolite (e.g. dihydroxyacetone phosphate and glyceraldehyde-3-phosphate); (iii) compounds that do not contribute to the carbon flux were not included in the reaction network (e.g. cofactors such as CoA is considered to have an infinite source); (iv) the network only includes physiologically occurring reactions (e.g. reactions known to proceed only under anaerobic conditions were not included).

The accumulation rates are calculated according to

$$r_i = \sum_j c_j x_j - \sum_k c_k x_k$$

where r_i is the accumulation rate of metabolite i, x_j the flux through reaction j, producing metabolite i with a stoichiometric coefficient c_j, and x_k is the flux through reaction k, consuming i with a stoichiometric coefficient c_k. The concentration of metabolites assumed to hold a pseudo steady state will be constant, that is $r_i = 0$. The accumulation rates of substrates, extracellular metabolites, and biomass were obtained experimentally. The set of balance equations can be written in matrix notation as $\boldsymbol{A}\cdot\boldsymbol{x} = \boldsymbol{r}$, where $\boldsymbol{A}$ is the $\boldsymbol{m} \times \boldsymbol{n}$ matrix of the stoichiometric coefficients, $\boldsymbol{x}$ the flux vector (with dimension $\boldsymbol{n}$) and $\boldsymbol{r}$ is the metabolite accumulation rate vector, $\boldsymbol{m}$-dimensional.

In our stoichiometric model, the number of metabolites ($\boldsymbol{m}$) is greater than the number of reactions ($\boldsymbol{n}$). $\boldsymbol{A}$ being a full rank matrix, the flux vector $\boldsymbol{x}$ can be calculated by means of the least squares solution to the equation [4].

The reactions, expressed in C-mole, are shown below. arrows (→) indicate physiologically irreversible reactions, while double arrows (↔) indicate reversible reactions. The model proved to be robust, confirmed by its condition number. The system was solved by Fluxanalyser [52] (kindly supplied by Steffan Klamt, Max Plank Institute for Dynamics of Complex Technical Systems, Magdeburg, Germany). Fluxanalyser does not provide an approximation to observed values but uses the observed values, unchanged, to predict experimentally inaccessible fluxes.

1. Glycerol + 0.333ATP + 0.333FAD → α-glycerophosphate + 0.333ADP + 0.333FADH
2. α-Glycerophosphate + 0.167ADP ↔ fructose-6-phosphate + 0.167ATP
3. Fructose-6-phosphate ↔ glucose-6-phosphate
4. α-Glycerophosphate + 0.333ADP + 0.333NAD → glyceraldehyde-3-phosphate + 0.333ATP + 0.333NADH
5. Glyceraldehyde-3-phosphate ↔ phosphoenolpyruvate
6. Phosphoenolpyruvate + 0.333ADP → pyruvate + 0.333ATP
7. Pyruvate + 0.333NAD → 0.667 acetyl-Co-A + 0.333CO_2 + 0.333NADH
8. Acetyl-Co-A + 2 oxaloacetate ↔ 3 isocitrate
9. Isocitrate + 0.167NADP ↔ 0.833 α-ketoglutarate + 0.167NADPH + 0.167CO_2
10. α-Ketoglutarate + 0.2NAD + 0.2ADP ↔ 0.8 succinate + 0.2CO_2 + 0.2NADH + 0.2ATP
11. Succinate + 0.25FAD ↔ malate + 0.25FADH
12. Malate + 0.25NAD ↔ oxaloacetate + 0.25NADH
13. Xylose-5-P + ribose-5-P ↔ 1.4 1,4 sedoheptulose-7-P + 0.6 glyceraldehyde-3-phosphate
14. 1,4-Sedoheptulose-7-P + 0.428 glyceraldehyde-3-phosphate ↔ 0.857 fructose-6-phosphate + 0.571 erythrose-4-P
15. 1.2 Fructose-6-phosphate + 0. glyceraldehyde-3-phosphate ↔ xylose-5-P + 0.8 erythrose-4-P
16. Ribulose-5-P ↔ ribose-5-P
17. Ribulose-5-P ↔ xylose-5-P
18. α-Ketoglutarate + 0.2 NH_4 + 0.2NADPH ↔ glutamate + 0.2NADP
19. Glutamate + 0.2NH_4 + 0.2ATP → glutamine + 0.2ADP
20. Glutamate + 0.2ATP + 0.4NADPH → proline + 0.2ADP + 0.4NADP
21. Glutamate + 0.5ATP + 0.1NADPH + 0.1NH_4 + 0.1CO_2 + 0.4 aspartate → 0.6 arginine + 0.5 α-ketoglutarate + 0.5ADP + 0.4 fumarate + 0.1NADP
22. Glutamate + 0.2 acetyl-Co-A + 0.3ATP + 0.2NADPH + 0.2NAD → 0.6 lysine + 0.5 α-ketoglutarate + 0.1CO_2 + 0.3ADP + 0.2NADP + 0.2NADH
23. Glyceraldehyde-3-phosphate + 1.67 glutamate + 0.333NAD → serine + 1.67 α-ketoglutarate + 0.333NADH
24. Serine + 0.671NAD → 0.67 glycine + 0.33CO_2 + 0.671NADH
25. Serine + 1.333NADPH + 0.333ATP → cysteine + 1.333NADP + 0.333ADP
26. Oxaloacetate + 1.25 glutamate → aspartate + 1.25 α-ketoglutarate
27. Aspartate + 0.25NH_4 + 0.5ATP → asparagine + 0.25ADP
28. Aspartate + 0.5ATP + 0.5NADPH → threonine + 0.5ADP + 0.5NADP
29. Aspartate + 0.5ATP + 0.5NADPH + 0.75 cysteine + 0.25175CO_2 + 0.75525NADH → 1.25 methionine + 0.75 pyruvate + 0.25NH_4 + 0.5ADP + 0.5NADP + 0.75525NAD
30. Threonine + 0.75 pyruvate + 0.25NADPH + 1.25 glutamate → 1.5 isoleucine + 0.25NH_4 + 0.25NADP + 0.25CO_2 + 1.25 α-ketoglutarate
31. Pyruvate + 1.667 glutamate → alanine + 1.667 α-ketoglutarate
32. 1.2 Pyruvate + 0.2NADPH + glutamate → valine + α-ketoglutarate + 0.2CO_2 + 0.2NADP
33. 1.2 Pyruvate + 0.2NADPH + 0.4 acetyl-Co-A + glutamate + 0.2NAD + 0.2ATP → 1.2 leucine + α-ketoglutarate + 0.2CO_2 + 0.2NADH + 0.2ADP + 0.2NADP + 0.2CO_2

34. 0.6 Phosphoenolpyruvate + 0.4 erythrose-4-P + 0.1NADPH + 0.1ATP + 0.5 glutamate → 0.9 phenylalanine + 0.5 α-ketoglutarate + 0.1CO_2 + 0.1ADP + 0.1NADP
35. 0.6 Phosphoenolpyruvate + 0.4 erythrose-4-P + 0.1NADPH + 0.1ATP + 0.5 glutamate + 0.1NAD → 0.9 tyrosine + 0.5 α-ketoglutarate + 0.1CO_2 + 0.1ADP + 0.1NADP
36. 0.6 Phosphoenolpyruvate + 0.4 erythrose-4-P + 0.1NADPH + 0.1ATP + 0.5 glutamine + 0.5 ribulose-5-P + 0.2ATP + 0.3 serine → 1.1 tryptophan + 0.1CO_2 + 0.3 α-glycerophosphate + 0.5 glutamate + 0.3 pyruvate + 0.2ADP + 0.1ADP + 0.1NADP
37. Ribulose-5-P + ATP + 0.2NH_4 + glutamine + 0.4NAD + 0.2NADPH + 0.2CO_2 → 1.2HYS + 0.2NADH + 0.2NADP + ADP + α-ketoglutarate
38. Glutamate + 0.2ATP + 0.2NADPH + glutamate → ornithine + 0.2ADP + 0.2NADP + α-ketoglutarate
39. Phosphoenolpyruvate + 0.333CO_2 → 1.333 oxaloacetate
40. 0.5 Ribose-5-P + 0.8ATP + 0.3 glycine + 0.4 aspartate + glutamine + 0.1NADH + 0.2CO_2 + 0.4 aspartate → AMP + 0.4 fumarate + 0.8ADP + glutamate + 0.1NAD + 0.4 fumarate
41. 0.5 Ribose-5-P + 0.9ATP + 0.3 glycine + 0.4 aspartate + glutamine + 0.1NADH + 0.2CO_2 + 0.1NAD + 0.5 glutamine → GMP + 0.5 glutamate + 0.1NADH + 0.9ADP + glutamate + 0.1NAD + 0.4 fumarate
42. 0.555 Glutamine + 0.555 ribose-5-P + 0.666ATP + 0.444 aspartate + 0.111NAD ↔ UTP + 0.666ADP + 0.555 glutamate + 0.111NADH
43. UTP + 0.555 glutamine + 0.111ADP → CMP + 0.111ATP + 0.555 glutamate
44. 0.0246AMP + 0.0246GMP + 0.0323UMP + 0.00295CMP + 0.34ATP → RNA + 0.34ADP
45. Amino acids → protein
46. 8 Acetyl-Co-A + 15ATP + 15NADPH + O_2 → palmitate + 15ADP + 15NADP
47. 0.167 Glucose-6-phosphate + 0.167ATP → polysaccharide + 0.167ADP
48. Polysaccharide → $\text{polysaccharide}_{\text{extracellular}}$
49. 2NADH + O_2 + 4ADP → 4ATP + 2NAD
50. 2FADH + O_2 + 2ADP → 2ATP + 2FAD
51. ATP → ADP
52. NADPH ↔ NADH
53. Arginine → urea + ornithine
54. Ornithine + aspartate + ATP → argininosuccinate
55. Argininosuccinate → fumarate + arginine
56. Urea → CO_2 + NH_4
57. Glyceraldehyde-3-phosphate + 2 arginine + 0.667 NADPH + 0.333 FAD → 3 clavulanic acid + 0.667 NADP + 0.333 FADH

References

[1] Reading C, Cole M. Clavulanic acid: a β-lactamase-inhibiting β-lactam from *Streptomyces clavuligerus*. Antimicrob Agent Chemother 1977;11:852–7.

[2] Jorgensen H, Nielsen J, Villadsen J, Mollgard H. Metabolic flux distribution in *Penicillium chrysogenum* during fed-batch cultivations. Biotechnol Bioeng 1995;46:117–31.

[3] Sauer U, Hatzimanikatis V, Hohmann H-P, Manneberg M, van Loon APGM, Bailey JE. Physiology and metabolic fluxes of wild-type and riboflavin-producing *Bacillus subtilis*. Appl Environ Microbiol 1996;62:3687–96.

[4] Vallino JJ, Stephanopoulos G. Flux determinations in cellular bioreaction networks: application to lysine fermentations. In: Sikdar SK, Bier M, Todd P, editors. Frontiers of bioprocessing. Boca Raton, FL: CRC Press; 1990. p. 205–19.

[5] Vallino JJ, Stephanopoulos G. Metabolic flux distribution in *Corynebacterium glutamicum* during growth and lysine overproduction. Biotechnol Bioeng 1993;41:633–46.

[6] de Hollander JA. Potential limitations in lysine production by *Corynebacterium glutamicum* as revealed by metabolic network analysis. Appl Microbiol Biotechnol 1994;42:508–15.

[7] Zhu Y, Rinzema A, Bonarius HPJ, Tramper J, Bol J. Microbial transglutaminase production by *Streptoverticillium mobaraense*: analysis of amino acid metabolism using mass balances. Enzyme Microb Technol 1998;23:216–26.

[8] Çalik P, Özdamar TH. Mass flux balance-based model and metabolic pathway engineering analysis for serine alkaline protease synthesis by *Bacillus licheniformis*. Enzyme Microb Technol 1999;24:621–35.

[9] Rozkov A, Avignone-Rossa CA, Ertl PF, Jones P, O'Kennedy RD, Smith JJ, et al. Characterization of the metabolic burden on *Escherichia coli* DH1 cells imposed by the presence of a plasmid containing a gene therapy sequence. Biotechnol Bioeng 2004;88:909–15.

[10] Stephanopoulos GN, Aristidou AA, Nielsen J. Metabolic engineering: principles and methodologies. California: Academic Press; 1998.

[11] Varma A, Boesch BW, Palsson BO. Biochemical production capabilities of *Escherichia coli*. Biotechnol Bioeng 1993;42:59–73.

[12] Savinell JM, Palsson BO. Optimal selection of metabolic fluxes for in vivo experimental determination. I. Development of mathematical methods. J Theor Biol 1992;155:201–14.

[13] Fang A, Keables P, Demain AL. Unexpected enhancement of ß-lactam antibiotic formation in *Streptomyces clavuligerus* by very high concentrations of exogenous lysine. Appl Microbiol Biotechnol 1996;44:705–9.

[14] Kasarenini S, Demain AL. A role for alanine in the ammonium regulation of cephalosporin biosynthesis in *Streptomyces clavuligerus*. J Ind Microbiol 1994;13:217–9.

[15] Romero J, Lirás P, Martín JF. Dissociation of cephamycin and clavulanic acid biosynthesis in *Streptomyces clavuligerus*. Appl Microbiol Biotechnol 1984;20:318–25.

[16] Madduri K, Stuttard C, Vining LC. Lysine catabolism in *Streptomyces* spp. is primarily through cadaverine: β-lactam producers also make α-aminoadipate. J Bacteriol 1989;171:299–302.

[17] Bushell ME, Fryday A. The application of materials balancing to the characterisation of sequential secondary metabolite formation in *Streptomyces cattleya* NRRL 8057. J Gen Microb 1983;129:1733–42.

[18] Kirk S, Avignone-Rossa CA, Bushell ME. Growth limiting substrate affects antibiotic production and associated metabolic fluxes in *Streptomyces clavuligerus*. Biotechnol Lett 2000;22:1803–9.

[19] Ives PR, Bushell ME. Manipulation of the physiology of clavulanic acid production in *Streptomyces clavuligerus*. Microbiol 1997;143:3573–9.

[20] Chen K-C, Lin Y-H, Wu J-Y, Hwang S-CJ. Enhancement of clavulanic acid production in *Streptomyces clavuligerus* with ornithine feeding. Enzyme Microb Technol 2003;32:152–6.

[21] Valentine BP, Bailey CR, Doherty A, Morris J, Elson SW, Baggaley KH, et al. Evidence that arginine is a later metabolic intermediate than ornithine in the biosynthesis of clavulanic acid by *Streptomyces clavuligerus*. J Chem Soc Chem Commun 1993;15:1210–1.

[22] Stirling I, Elson SW. Studies on the biosynthesis of clavulanic acid. II. Chemical degradations of ^{14}C-labelled clavulanic acid. J Antibiot 1979;32:1125–9.

[23] Townsend CA, Mao S-S. Clavulanic acid biosynthesis: the stereochemical course of beta-lactam formation from chiral glycerol. J Chem Soc Chem Commun 1987:86–9.

[24] Khaleeli N, Li R, Townsend CA. Origin of the β-lactam carbons in clavulanic acid from an unusual thiamine pyrophosphate-mediated reaction. J Am Chem Soc 1999;121:9223–4.
[25] Avignone Rossa C, White CJ, Kuiper A, Postma PW, Bibb M, Teixeira de Mattos MJ. Carbon flux distribution in antibiotic-producing chemostat cultures of *Streptomyces lividans*. Metab Eng 2002;4:138–50.
[26] Foulstone M, Reading C. Assay of amoxicillin and clavulanic acid, the components of augmentin, in biological fluids with high performance liquid chromatography. Antimicrob Agent Chemother 1982;22:753–62.
[27] Herbert D, Phipps PJ, Strange RE. Chemical analysis of microbial cells. In: Norris JR, Ribbons DW, editors. Methods in microbiology, vol. 5b. London: Academic Press; 1971. p. 209–34.
[28] Lowry OH, Rosebrough NJ, Farr AL, Randall RJ. Protein measurement with the Folin phenol reagent. J Biol Chem 1951;193:265–76.
[29] Dubois M, Gilles K, Hamilton JK, Rebers PA, Smith F. Colorimetric method for the determination of sugars and related substances. Anal Chem 1956;28:350–6.
[30] Bligh EG, Dyer WJ. A rapid method of total lipid extraction and purification. Can J Biochem Biophys 1959;37:911–7.
[31] Burton K. A study of the conditions and mechanism of the diphenylamine reaction for the colorimetric estimation of deoxyribonucleic acid. Biochem J 1959;62:314–23.
[32] Herbert D, Phipps PJ, Strange RE. In: Norris JR, Ribbons DW, editors. Chemical analysis of microbial cells, vol. 5b. London: UK Academic Press; 1971. p. 308–29.
[33] Shahab N, Flett F, Oliver SG, Butler PR. Growth rate control of protein and nucleic acid content in *Streptomyces coelicolor* A3(2) and *Escherichia coli* B/r. Microbiol 1996;142:1927–35.
[34] Olukoshi ER, Packter NM. Importance of stored triacylglycerols in Streptomyces: possible carbon source for antibiotics. Microbiol 1994;140:931–43.
[35] Gesheva V, Rachev R, Bojkova S. Fatty acid composition of Streptomyces hygroscopicus strains producing antibiotics. Lett Appl Microbiol 1997;24:109–12.
[36] Salas JA, Quiros LM, Hardisson C. Pathways of glucose catabolism during germination of Streptomyces spores. FEMS Microbiol Lett 1984;22:229–33.
[37] Dekleva ML, Strohl WR. Activity of phosphoenolpyruvate carboxylase of an anthracycline-producing streptomycete. Can J Microbiol 1988;34:1241–6.
[38] Alves, AM. Regulation of glucose metabolism in the actinomycetes *Amycolatopsis methanolica* and *Streptomyces coelicolor* A3(2). Doctoral Thesis, University of Groningen, 1997.
[39] Holms H. Flux analysis and control of the central metabolic pathways in *Escherichia coli*. FEMS Microbiol Rev 1996;19:85–116.
[40] Hodgson JE. Primary metabolism and its control in Streptomycetes: a most unusual group of bacteria. Adv Microbial Physiol 2000;42:47–238.
[41] Moat AG, Foster JW. Microbial physiology. 3rd ed. New York, USA: Wiley-Liss; 1995.
[42] Bascarán V, Hardisson C, Braña AF. Regulation of nitrogen catabolic enzymes in *Streptomyces clavuligerus*. J Gen Microbiol 1983;135:2465–74.
[43] de la Fuente JL, Martín JF, Lirás P. New type of hexameric ornithine carbamoyltransferase with arginase activity in the cephamycin producers *Streptomyces clavuligerus* and *Nocardia lactamdurans*. Biochem J 1996;320:173–9.
[44] Jensen SE, Paradkar AS. Biosynthesis and molecular genetics of clavulanic acid. Ant van Leeuwen 1999;75:125–33.
[45] Elson SW, Baggaley KH, Davison M, Fulston M, Nicholson NH, Risbridger GD, et al. The identification of three new biosynthetic intermediates and one further biosynthetic enzyme in the clavulanic acid pathway. J Chem Soc Chem Commun 1993;13:1212–4.
[46] Hodgson JE, Fosberry AP, Rawlinson NS, Ross HNM, Neal RJ, Arnell JC, et al. Clavulanic acid biosynthesis in *Streptomyces clavuligerus*: gene cloning and characterization. Gene 1995;166:49–55.
[47] McDermott JF, Lethbridge G, Bushell ME. Estimation of the kinetic constants and elucidation of trends in growth and erythromycin production in batch and continuous cultures of *Saccharopolyspora erythraea* using curve-fitting techniques. Enzyme Microb Technol 1993;15:657–63.
[48] Mayer AF, Deckwer WD. Simultaneous production and decomposition of clavulanic acid during *Streptomyces clavuligerus* cultivations. Appl Microbiol Biotechnol 1996;45:41–6.
[49] Portais J-C, Delort A.-M. Carbohydrate cycling in microorganisms: what can 13C-NMR tell us? FEMS Microbiol Revs 2002;26:375–402.
[50] Mendz G, Hazell SL. The urea cycle of *Helicobacter pylori*. Microbiol 1996;142:2959–76.
[51] Garcia-Dominguez M, Martin JF, Liras P. Characterization of sugar uptake in wild-type *Streptomyces clavuligerus*, which is impaired in glucose uptake, and in a glucose-utilizing mutant. J Bacteriol 1989;171:6808–14.
[52] Klamt S, Stelling J, Ginkel M Gilles, editors. FluxAnalyzer: exploring structure, pathways, and flux distributions in metabolic networks on interactive flux maps. Bioinformatics 2003;19:261–9.